

Energy Recovery from Garden and Park Waste by Hydrothermal Carbonization with Process Water Recycling

Published as part of ACS Sustainable Chemistry & Engineering *virtual special issue* "Sustainable Energy and CO₂ Conversion—Angel Irabien Festschrift."

Ricardo Paul Ipiales, Diana Pimentel-Betancurt, Elena Diaz, Angeles de la Rubia, Juan J. Rodríguez,* and Angel F. Mohedano*



Cite This: <https://doi.org/10.1021/acssuschemeng.3c08438>



Read Online

ACCESS |

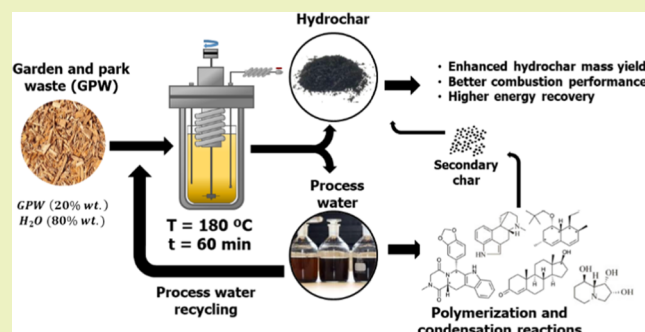
Metrics & More

Article Recommendations

Supporting Information

ABSTRACT: This study aims to obtain a carbonaceous material with suitable properties to be used as a solid biofuel by recycling process water from hydrothermal carbonization (HTC) of garden and park waste (GPW). The research is focused on maximizing mass yield and energy recovery as well as facilitating the treatment of the liquid fraction throughout reusing cycles of the liquid fraction. Process water recycling moderately improved the mass performance of the hydrochar, resulting in a higher energy recovery of almost 20 percentage points compared with that achieved (less than 79%) with conventional HTC (GPW + freshwater feed). An improvement in char fuel quality was observed, showing more suitable morphological, physical, and chemical characteristics, higher reactivity and combustion temperature, and lower probability of ash sintering. Successive process water reuse cycles allowed some increase in energy yield but, at the same time, degraded the quality of hydrochar as a biofuel. Process water composition showed an increase in chemical oxygen demand and total organic carbon, which almost doubled after three successive reuse cycles. The concentration of volatile fatty acids increased around 5-fold (up to 20 g L⁻¹), with acetic acid accounting for 85% of the total. Subsequent anaerobic digestion of the process water removed up to 75% of the COD and yielded a biogas with high methane content (225–302 N mL CH₄ g⁻¹ COD_{added}). Recycling of the process water significantly improved the total energy recovery (hydrochar + methane) to 90% after a single recycling, compared to 84% achieved with conventional HTC and subsequent anaerobic treatment of the resulting process water.

KEYWORDS: anaerobic digestion, garden and park waste, hydrochar, hydrothermal carbonization, process water recycling



1. INTRODUCTION

Nowadays, sustainable energy production and waste recovery are two of the most important current challenges, requiring strategies that effectively link these two objectives. Hydrothermal carbonization (HTC) is a promising technology capable of transforming biomass waste with poor energy characteristics into a valuable carbonaceous solid, called hydrochar, with higher energy value, chemical stability, and harmless character.¹ Hydrochar is an ideal candidate as a biofuel,² soil amendment,³ carbon sequestration agent,⁴ or activated carbon precursor.⁵ HTC is carried out at moderate temperatures (180–250 °C), low to moderate residence time (5–240 min), and autogenous pressure. The presence of water during HTC plays a crucial role in facilitating the removal of thermally unstable organic species, inorganic matter, and intermediate compounds, transferring them to the liquid fraction, usually called process water (PW).

Hydrochar is formed by the dehydration and decarboxylation of the starting biomass material, releasing H₂O and CO₂ and increasing the C content of the resulting solid. This solid–solid transformation step yields a primary hydrochar, accounting for up to 60 wt % of the total hydrochar mass yield (Y_{HC}) obtained. Recent studies have reported that organic species solubilized in the process water tend to react with each other through polymerization, condensation, and Maillard reactions, leading to the formation of more complex and high-molecular-weight compounds.⁶ These structures precipitate as solid particles within the primary hydrochar, giving rise to what

Received: December 27, 2023

Revised: February 29, 2024

Accepted: March 1, 2024

Table 1. Analytical Characterization of GPW and Hydrochars^{a,b} (wt %, Dry Basis)

	GPW	HC	HC1	HC2	HC3
Y_{HC}		75.5 (3.4) ^a	79.3 (7.8) ^a	89.3 (4.7) ^b	85.5 (2.0) ^b
VM	76.5 (0.6) ^a	67.1 (0.2) ^b	74.1 (0.5) ^c	77.4 (0.4) ^a	78.9 (0.4) ^d
FC	18.4 (0.2) ^a	29.7 (0.2) ^b	18.8 (0.2) ^a	15.3 (0.3) ^c	13.8 (0.2) ^d
ash	5.1 (0.2) ^a	3.2 (0.1) ^b	7.1 (0.1) ^c	7.3 (0.2) ^c	7.3 (0.2) ^c
wax	5.8 (0.2) ^a	6.7 (0.1) ^a	9.1 (0.2) ^b	8.9 (0.2) ^a	9.3 (0.3) ^a
hemicellulose	25.2 (1.2) ^a	7.6 (0.2) ^b	0.2 (0.1) ^c	0.2 (0.0) ^c	0.1 (0.1) ^d
cellulose	41.4 (2.3) ^a	43.3 (0.5) ^a	46.8 (0.5) ^b	43.2 (1.0) ^a	43.6 (0.2) ^a
lignin	22.5 (0.6) ^a	38.8 (1.0) ^b	38.8 (0.3) ^b	40.2 (0.8) ^b	42.9 (0.6) ^c
C	46.9 (0.5) ^a	49.8 (0.2) ^b	51.9 (0.1) ^c	51.2 (0.3) ^d	52.2 (0.1) ^c
H	6.1 (0.1) ^a	5.3 (0.1) ^b	5.8 (0.1) ^c	5.1 (0.2) ^b	5.3 (0.1) ^b
N	0.9 (0.1) ^a	1.3 (0.1) ^b	1.1 (0.1) ^c	1.7 (0.1) ^d	1.6 (0.1) ^c
S	0.4 (0.1) ^a	0.2 (0.1) ^b	0.1 (0.0) ^c	0.1 (0.0) ^c	0.1 (0.0) ^c
O	40.6 (0.1) ^a	40.2 (0.2) ^b	34.0 (0.2) ^c	34.6 (0.5) ^c	33.5 (0.1) ^c

^aAverage values with standard deviations (in parentheses). ^bMeans with a different superscript significantly differ ($p < 0.05$).

is called secondary hydrochar, which can represent up to 40 wt % of the total weight of the hydrochar produced. The rate of secondary hydrochar production is strictly dependent on the characteristics of the starting biomass. Carbohydrates in the presence of amino acids or N-heterocyclic compounds can yield secondary hydrochar and be incorporated into primary hydrochar.⁷ On the other hand, Pecchi et al. indicate that lipid-rich organic compounds can enhance secondary hydrochar by up to 50% in the presence of sugars and/or carbohydrates.⁸ Meanwhile, Yang et al.⁷ suggest that this phenomenon is attributed to lipids forming a wide variety of short-chain organic acids that can yield long-chain fatty acids and be incorporated into hydrochar.⁸ Additionally, previous studies highlight that O- and N-bearing aromatic compounds are also involved in secondary hydrochar formation, and their presence in the process water could shift the balance toward secondary hydrochar formation.^{9,10}

Process water contains inorganic matter as well as nutrients, and a high fraction of the initial C (up to 60% of the total carbon from the feedstock), as soluble organic compounds such as low-chain acids (formic, acetic, lactic, and propionic), sugars (glucose, fructose, and xylose), furans (furfural and 5-HMF) and phenols, in addition to metal ions and nutrients such as Mg^{2+} , Ca^{2+} , K^+ , NH_4^+ or PO_4^{3-} .^{11,12} Different approaches are proposed in the literature to obtain value-added products from the process water or to mitigate the potential negative environmental impact of those liquid wastes.^{13,14} Anaerobic digestion (AD) stands out as one of the most investigated complementary ways for effective recovery of the process water from HTC. Several studies report high methane production (200–330 N mL CH_4 g⁻¹ COD_{added}) as well as significant organic matter removal (40–70%).^{11,15} However, process water biodegradability as well as methane production and organic matter removal are closely dependent on the biomass feedstock and HTC operating conditions. Gaur et al.¹⁶ report that increasing the working temperature (>200 °C) significantly decreases further methane production from the resulting PW by up to 70% and organic matter removal by 50%. In addition, biomass rich in carbohydrates and proteins tends to yield recalcitrant compounds, which even inhibit methanogenic organisms.^{17,18}

A new potentially feasible and advantageous alternative to deal with PW is simply to recycle it back to the HTC process.^{19–21} This can be an effective approach to reduce freshwater consumption in the recovery of low-moisture

biomass, such as lignocellulosic biomass, by HTC.²² The process water obtained in the initial cycle can be reused as a reaction medium, thus closing the water consumption cycle. In addition, as indicated before, the presence of a high concentration of organic compounds in the liquid fraction can promote parallel reactions such as condensation, polymerization, and Maillard reactions, leading to higher Y_{HC} from the formation of secondary hydrochar.^{23,24} Several studies have shown that recycling of process water enhances dehydration and decarboxylation reactions, resulting in a hydrochar with lower atomic H/C and O/C ratios,^{25,26} which, especially the last, favors a more hydrophobic character.²³ In addition, the formation of unsaturated bonds is also favored, suggesting the occurrence of aromatization and polymerization reactions.¹⁹ Higher occurrence of decarboxylation and dehydration reactions would lead to a higher C content and, consequently, also a higher heating value of the resulting hydrochar compared to the commonly obtained by conventional HTC with fresh water.

On the contrary, recycling of process water favors higher ash, N, S, nutrients, and volatile matter (VM) contents of the hydrochar,^{21,22} which could reduce its potential interest as biofuel. Well-known problems associated with those features are ash sintering, causing fouling and slagging in boilers,²⁷ NO_x and SO_2 formation during combustion, as well as corrosion problems.²⁸ High VM content can lead to rapid consumption of the solid material, incomplete combustion, and explosion risks.²⁹ The potential use of hydrochar as biofuel is established in ISO/TS 17225-8 standards,³⁰ which limit ash (<10 wt %), N (<3 wt %), S (<0.5 wt %), VM (<75 wt %), and HHV (>17 MJ kg⁻¹) values.

The formation of secondary hydrochar, due to high solubilization of organic matter in the liquid fraction, can result in lower production of primary hydrochar, which presents high stability and energy density,⁶ so efforts should focus on improving HTC to maximize and balance the production of both primary and secondary hydrochar addressed to improve the energy recovery and obtain a final product with the best suitability regarding the required application. The intensity of PW recycling (number of successive cycles) could play an important role in that sense since it affects the accumulation of organic acids, refractory compounds, metal ions, and heavy metal loads in the reaction medium. The aim of this work is to analyze the effect of PW recycling on HTC of garden and park waste (GPW) as

representative lignocellulosic waste. The study is focused on evaluating the improvement of both the mass yield to hydrochar and the characteristics of the resulting hydrochar for use as an industrial biofuel. Additionally, we explored the treatment of process water by anaerobic digestion to reduce the organic load of the final effluent and recover energy by producing methane-rich biogas.

2. MATERIALS AND METHODS

2.1. Feedstock Characterization. GPW was collected from the Migas Calientes Composting Plant located in Madrid (Spain). The feedstock was dried in an oven at 105 °C to a constant weight, with a total solids (TS) content of ~96 wt %. Then GPW was ground, sieved to less than 3 mm, and stored in closed containers at room temperature until HTC experiments. Representative characteristics of GPW are shown in Table 1.

2.2. HTC with PW Recycling. HTC experiments were conducted in an electrically heated 4 L ZipperClave pressure vessel. GPW, with a moisture content of ~5%, was mixed with deionized water (DW) at a GPW:DW ratio of 20:80 wt % to ensure hydrothermal conditions. In the first HTC cycle, the reaction mixture (GPW and DW) was heated at 3 °C min⁻¹ to 180 °C and maintained at this temperature for 1 h under vigorous stirring (180 rpm). After that time, the reactor was cooled by an internal coil using tap water with a cooling rate of 10 °C min⁻¹. The resulting slurry (hydrochar + process water) was separated by centrifugation (Ortoalresa; Madrid, Spain) at 8000 rpm for 10 min and filtration (0.45 μm), and the process water (PW) was stored at 4 °C for characterization and recycling in the subsequent HTC runs. The wet hydrochar was dried at 105 °C for 24 h, ground in an air atmosphere, and sieved (<250 μm) for further characterization. The PW obtained after each HTC run was used in subsequent ones, conducted at the same operating conditions (180 °C for 1 h and a GPW-to-PW ratio of 20:80 wt %). The HTC runs using deionized water and process water recycling were performed in triplicate.

The hydrochar and process water obtained from the first cycle (using DW) were designated as HC and PW; the hydrochars and process waters obtained in subsequent runs, where PW was recycled, were labeled following the number of process water reuse cycles performed (HC1, HC2, HC3, PW1, PW2, and PW3, respectively).

2.3. Feedstock and Hydrochar Characterization. The elemental composition (C, H, N, and S) was determined using a CHNS analyzer (LECO CHNS-932; Geleen, The Netherlands). Proximate analysis (VM, fixed carbon (FC), and ash content) was performed using a Discovery SDT thermogravimetric analyzer (TG 209, F3, Netzsch; Selb, Germany) according to the ASTM-D7582 method.³¹ The oxygen (O) content was assessed by the difference between C, H, N, and S and the ash content. Mineral and heavy metal elements were quantified by inductively coupled plasma atomic emission spectroscopy (ICP-OES) on an Elan 6000 Sciex (PerkinElmer; Santa Clara, CA) instrument. The fiber structure (wax, hemicellulose, cellulose, and lignin) of GPW and hydrochars was analyzed according to ISO 16472:2006 and ISO 13906:2008.³² The morphology of hydrochars was assessed by scanning electron microscopy (SEM) in a Hitachi S-3000N apparatus (Hitachi Ltd., Tokyo, Japan). The images were obtained using a secondary electron (SE) and backscattered electron (BSE) detector in the high vacuum mode under an acceleration voltage of 20 kV. The surface composition and functional groups of hydrochar were studied by Fourier transform infrared spectroscopy (FTIR) using an FTIR Bruker IFS66v spectrophotometer (Bruker Corporation, Billerica, MA), following the KBr disk method having a resolution of 4 cm⁻¹ from 4000 to 550 cm⁻¹ and 250 scans. Temperature-programmed desorption (TPD) was used to assess the oxygen surface groups on the hydrochar. TPD runs were carried out using 0.1 g of GPW or hydrochar. Samples were heated to 900 °C at 10 °C min⁻¹ in a vertical quartz tube under continuous N₂ flow of 1 N L min⁻¹. The amounts of CO₂ and CO evolved were analyzed by a nondispersive infrared sensor in a Siemens model Ultramat 22 equipment (Siemens

Aktiengesellschaft, Munich, Germany). All of the analyses were performed in triplicate.

2.4. Combustion-Related Properties of Hydrochars. Thermogravimetric (TG) and derivative thermogravimetry (DTG) analyses were performed in a thermogravimetric analyzer (Discovery SDT 650). The samples were heated from 25 to 900 °C at 10 °C min⁻¹ under a 100 N mL min⁻¹ continuous air flow. Ignition temperature (*T_i*), burnout temperature (*T_b*), and peak temperature of the maximum loss weight (*T_m*) are characteristic parameters reflecting the thermal behavior of fuels during combustion. The comprehensive combustibility index (CCI, eq 1) quantifies the combustion potential of biofuels, while fuel ratio (FR, eq 2) delineates the combustion intensity and stability.³³

$$CCI \text{ (min}^{-2} \cdot \text{°C}^{-3}\text{)} = \frac{\left(\frac{dw}{dt}\right)_{\max} - \left(\frac{dw}{dt}\right)_{\text{mean}}}{T_i^2 \cdot T_b} \quad (1)$$

where $(dw/dt)_{\max}$ and $(dw/dt)_{\text{mean}}$ refer to the maximum and average weight loss rates, respectively.

$$FR = \frac{FC \text{ (\%)}}{VM \text{ (\%)}} \quad (2)$$

Slagging and fouling indexes were calculated based on the ash composition according to the equations reported by Masiá et al.³⁴ and modified by Cao et al.³⁵ These indexes (acid–base ratio (*R_{b/a}*), fouling index (FI), slagging index (SI), and alkali index (AI)) are listed in Table S1.

2.5. Process Water Characterization. The process water samples were characterized by measuring pH (Crison 20 Basic pH-meter), TS, and volatile solids (VS) according to 2540B and 2540E methods, respectively.³⁶ Soluble chemical oxygen demand (SCOD) was determined using the APHA 5220D method.³⁶ Total organic carbon (TOC) was measured using a TOC-VCPN analyzer (Shimadzu TOC Analyzers, Spain). Individual volatile fatty acid (VFA) concentrations, from acetic to heptanoic (including iso-forms), were determined by gas chromatography with a flame ionization detector (GC-FID) in a Varian 430-GC instrument.³⁷ Total Kjeldahl nitrogen (TKN) and ammonia nitrogen (NH₃-N) were determined according to standard methods 4500D and 4500E, respectively (APHA, 2005). Organic nitrogen (Org-N) was calculated as the difference between TKN and NH₃-N. Chemical species in PW were analyzed by gas chromatography/ion-trap mass spectrometry (GC-MS) in a CP-3800/Saturn 2200 instrument equipped with a Varian CP-8200 autosampler injector and a Carbowax/Divinylbenzene Yellow Green solid-phase microextractor using a factor Four VF-5 MS capillary column.³⁸ The identification was made by correspondence with the database of data from the NIST mass spectral library. All of the analyses were performed in triplicate.

2.6. Anaerobic Digestion of PW. Anaerobic digestion runs were conducted in batch using 120 mL glass serum vials. The inoculum concentration was set at 15 g VS L⁻¹, and the inoculum-to-substrate ratio (ISR) was maintained at 2, on a VS basis. The granular anaerobic sludge came from an industrial digester treating brewery wastewater under mesophilic conditions (35 °C). This inoculum showed the following characteristics: 54.5 (0.9) g of TS L⁻¹, 45.7 (0.2) g of VS L⁻¹, and 73.5 (0.2) g of COD L⁻¹. A basal medium containing macro and micronutrients was prepared and subsequently introduced into the system, as described elsewhere.³⁹ The vials were filled up to 60 mL with DW, closed with rubber stoppers, and flushed with nitrogen for 2 min to ensure anaerobic conditions. They were kept in a thermostatic water bath at mesophilic temperature of 35 °C under shaking at an equivalent of 150 rpm. AD experiments were monitored using 10 vials (for each substrate): 3 for biogas measurements (volume and composition), and the other 7 were sacrificed to monitor anaerobic digestion operating variables such as pH, SCOD, TOC, and VFA. Substrate-free samples were used to establish the background biogas level of the inoculum, while starch-fed control samples (soluble potato starch; Panreac), both in triplicate, confirmed the inoculum activity, producing 350 (10) mL

STP CH_4 g^{-1} COD_{added}. The biogas composition (H_2 , CO_2 , CH_4 , and H_2S) was analyzed by a gas chromatograph (Thermo Scientific Trace 1300; Villebon, France) equipped with a thermal conductivity detector (TCD) using an 8 ft \times 1/8 in SS column packed with HayeSep Q 80/100 mesh.³⁸

2.7. Energy Recovery. The HHV of feedstock and hydrochars was estimated using the Schuster equation (eq 3), while the yields to hydrochar (Y_{HC}) and the process water yield (Y_{PW}) were calculated from eqs 4 and 5, respectively. The Y_{PW} is defined as the mass (organic and inorganic) in total solids transferred from GPW to the process water.

$$\text{HHV (MJ kg}^{-1}\text{)} = 0.3491 \cdot \text{C} + 1.033 \cdot \text{H} + 0.1005 \cdot \text{S} - 0.0151 \cdot \text{N} - 0.103 \cdot \text{O} - 0.0211 \cdot \text{ash} \quad (3)$$

$$Y_{\text{HC}} (\%) = \frac{W_{\text{HC}}}{W_{\text{GPW}}} \times 100 \quad (4)$$

$$Y_{\text{PW}} (\%) = \frac{\text{TS} \cdot V_{\text{PW}}}{W_{\text{GPW}}} \times 100 \quad (5)$$

where W_{HC} and W_{GPW} correspond to the mass (g) of the hydrochar and the starting feedstock, respectively, both on a dry basis. TS (g L^{-1}) is the total solids concentration in the process water, and V_{PW} (L) is the final volume recovered by filtration.

The specific methane production (SMP) ($\text{Nm}^3 \text{CH}_4 \text{ kg}^{-1} \text{COD}$) from the anaerobic digestion of PW was converted into HHV_{PW} using eq 6.

$$\text{HHV}_{\text{PW}} (\text{MJ kg}^{-1}) = 39.8 \cdot \text{SMP} \cdot \frac{\text{COD}}{\text{TS}} \quad (6)$$

where 39.8 is the higher heating value of methane (MJ Nm^{-3}) and COD is the chemical oxygen demand of process water (g L^{-1}).

The energy yield ascribed to hydrochar (E_{yield}) was calculated as the ratio between the HHV of hydrochar (HHV_{HC}) and that of GPW (HHV_{GPW}), considering the hydrochar mass yield (eq 7).

$$E_{\text{yield}} (\%) = \frac{Y_{\text{HC}} \cdot \text{HHV}_{\text{HC}}}{\text{HHV}_{\text{GPW}}} \times 100 \quad (7)$$

The total energy recovery associated with the products of the whole process (hydrochar from HTC plus methane from further anaerobic digestion of the resulting process water) was calculated by eq 8.

$$E_{\text{recovery}} (\text{MJ kg}^{-1}) = \text{HHV}_{\text{HC}} \cdot Y_{\text{HC}} + \text{HHV}_{\text{PW}} \cdot Y_{\text{PW}} \quad (8)$$

The distribution of carbon in the hydrochar and in the process water was determined by performing a mass balance, following eqs 9 and 10:

$$X_{\text{HC}} (\%) = \frac{C_{\text{iHC}} \cdot W_{\text{HC}}}{C_{\text{iGPW}} \cdot W_{\text{GPW}}} \times 100 \quad (9)$$

$$X_{\text{PW}} (\%) = \frac{C_{\text{iPW}} \cdot W_{\text{PW}}}{C_{\text{iGPW}} \cdot W_{\text{GPW}}} \times 100 \quad (10)$$

where C_i is the carbon content in the hydrochar (HC), process water (PW), or garden and park waste (GPW) and W_{HC} , W_{PW} , and W_{GPW} are the mass of hydrochar, process water (as total solids) recovered after filtration, and garden and park waste, respectively. The C content in the gas phase was calculated by the difference.

2.8. Statistical Analysis. Characterization tests of hydrochar and process water were made in triplicate, and the corresponding analysis of variance (ANOVA) was performed using GraphPad Prism 6.00 software. The minimum significant Fisher difference (Fisher LSD) was calculated with a confidence level of 0.05. The values in the tables are accompanied by the standard deviation in parentheses.

3. RESULTS AND DISCUSSION

3.1. Effect of Process Water Recycling on Hydrochar Characteristics. Table 1 shows the analytical characterization of GPW and the hydrochars obtained after each HTC test. The percentage of total solids in the hydrochars, after filtering and centrifuging the reaction medium, reached around 75 wt %, with no significant variations observed between the hydrochars obtained using demineralized water or process water. In the first run, conducted by the conventional HTC process (GPW + DW), the less stable components of the GPW, mainly VM and hemicellulose, underwent hydrolysis and were transferred to the process water, namely, PW. The mass yield to hydrochar (Y_{HC}) in that first run was close to 76 wt %. Hemicellulose, which was almost completely removed, is a plant cell wall component in lignocellulosic biomass and exhibits reduced thermal stability under hydrothermal conditions.⁴⁰ The FC content increased from 18 wt % in the GPW to 30 wt % in the resulting hydrochar (HC), while the ash content decreased by more than 35% (5.1 wt % in GPW vs 3.2 in HC). Recycling of the process water resulted in a significant improvement of hydrochar yield from 76 wt % to almost 90 wt % after the two following HTC runs performed with recycled PW. The small decrease from the second to the third PW-recycling run does not appear significant, in principle, looking not only at the average values but also at the standard deviations, although further insight would be needed to better clarify this issue. It could be expected that as the process water is recycled, a higher hydrochar mass yield would be observed. However, in the present work, from the third cycle onward, a constant value is reached, even lower than that obtained in the previous cycle. Other studies have also observed constant values after a certain number of process water recycles. Thus, Volpe et al.⁴¹ observed a stable value in the hydrochar mass yield after 3 process water recycles, similar to those found in this study, while Köchermann et al.⁴² observed a constant value after 8 process water recycles. It is important to note that the process water continues to be enriched in organic matter as the number of recycles increases. Proximate analyses revealed that the VM and ash contents of the hydrochar decreased with respect to those of the starting GPW in the first HTC run (with DW), and then both underwent significant increases after the first run with recycled PW, especially in the case of ashes. Stabilization of the ash content was observed in the successive PW-recycling runs, whereas some further increase of VM took place, up to even higher values than those of the waste feedstock. The FC underwent a quite significant raise from the starting GPW to the hydrochar obtained after the first HTC run, but then recycling of PW in the successive ones led to a monotonical decrease, yielding a final value 25% lower than that of the own raw waste. However, the meaning of the so-called FC and the way it is determined must be considered. Since the FC is defined as the difference between VM and ash as a percentage, increasing the ratio of VM and ash in hydrochar decreases the corresponding FC in hydrochar, even though the fixed carbon content may not vary in the reaction cycles. In fact, the elemental carbon content in HC3 hydrochar is 11.3% higher than that of GPW and almost 14% higher on an ash-free basis, mainly due to the increase in the VM content. The increase in VM content could be explained by the presence of soluble organic components resulting during conventional HTC (initial DW medium), which could act as intermediates in the formation of secondary hydrochar.⁶ In

addition, these soluble components could promote the hydrolysis of GPW constituents.²⁵ Fiber analysis showed an increase in wax content from 7 to 9 wt %, especially due to the combination of aliphatic polymers and VFA, which could have been formed during secondary polymerization, recondensation, and Maillard reactions of solubilized organic components.^{43,44} A clear increase in evolution can be observed for lignin, the C-richest constituent of lignocellulosic biomass. Its value increases in each HTC run and finally almost doubles in HC3 compared to that of the starting GPW. Meanwhile, the cellulose values show almost stable behavior. Some partial transfer of cellulose oligomers and monomers to the process water can take place through possible reactions with soluble organic components. Both cellulose and lignin tend to hydrolyze under hydrothermal conditions at temperatures of 200 and 220 °C, respectively,⁴⁵ although some lignin components could hydrolyze at lower temperatures, releasing lignin-derived monomers into the process water.^{46,47} The increase in ash content can be attributed to the large presence of dissolved metals, mainly Ca and K, which eventually precipitate in the hydrochar as the number of cycles increases (Table S2).^{48,49}

As indicated above, the elemental analyses yielded an increase in the average C content of the hydrochars in the runs performed with recycled PW with respect to the conventional HTC one. The final HC3 yielded more than 56% C on an ash-free basis, which compares well and even favorably with sub-bituminous coals commonly used in power generation. The H and O content showed a significant decrease, ascribed to the dehydration and decarboxylation reactions undergone by the precursor.⁵⁰ The presence of soluble organic compounds in the process water promotes the occurrence of reactions with carboxylic (R-C=O), ester (COOR), ether (R-OR), and alcohol (R-OH) groups of the lignocellulosic feedstock and the hydrochar formed. These compounds can act as Lewis bases donating electrons from soluble organic compounds, while H⁺ is a Lewis acid accepting electrons.^{51–53} This process enhances the cleavage of ethers and esters, promoting the hydrolysis of organic species in the remaining solid. The evolution of the atomic H/C and O/C ratios is also consistent with carbonization. The N content of the HC increased with respect to the GPW after conventional HTC, and a further increase in the recycled PW runs was observed. Previous studies have reported that N-bearing compounds (heterocyclic and aromatic) are intermediates in the formation of secondary hydrochar.^{18,22} In contrast to N, the S content decreased from the starting GPW to successive hydrochars. Low S content is a common advantage of biochars from lignocellulosic precursors.

Table 2 shows the main properties of hydrochars regarding potential use as a biofuel. The HHV increased moderately with respect to the starting GPW, consistently with the higher C and lower O content. The energy recovery associated with the hydrochar product (E_{yield}) increased significantly in the HTC runs using recycled PW with respect to the conventional one (initiated with DW): HC1 (~15%), HC2 (~22%), and HC3 (~21%) increase with respect to HC. According to ISO 17225-8,³⁰ HC and HC1 yielded characteristics suitable for industrial use as biofuels (HHV > 17 MJ·kg⁻¹, N < 3 wt %, S < 0.5 wt %, VM < 75 wt %, and ash < 10 wt %). In particular, the HHV is well above the lower limit of the standard, with a value of 21.3 MJ·kg⁻¹, which means 23 MJ·kg⁻¹ on an ash-free basis. This is also the case of HC2 and HC3, except for VM content, somewhat higher than the given in the guideline. However, in

Table 2. Combustion-Related Issues of Feedstock and Hydrochars from the HTC Runs and Energy Recovery Values^{a,b}

	GPW	HC	HC1	HC2	HC3
HHV (MJ kg ⁻¹)	18.7 (0.3) ^a	19.5 (0.1) ^a	21.3 (0.1) ^b	20.1 (0.4) ^c	20.9 (0.0) ^b
E_{yield} (%)		78.7 (0.3) ^a	90.3 (0.3) ^b	96.0 (0.5) ^c	95.6 (0.4) ^c
$R_{\text{b/a}}$	1.1 (0.0) ^a	0.9 (0.1) ^a	1.2 (0.1) ^a	1.6 (0.1) ^b	1.8 (0.2) ^b
SI	0.5 (0.0) ^a	0.1 (0.0) ^b	0.1 (0.0) ^b	0.2 (0.0) ^b	0.2 (0.1) ^b
FI	0.7 (0.0) ^a	0.3 (0.0) ^b	0.3 (0.0) ^b	1.4 (0.0) ^c	2.1 (0.2) ^d
AI	3.0 (0.2) ^a	1.5 (0.1) ^b	1.3 (0.0) ^b	4.3 (0.2) ^c	5.5 (0.2) ^d
T_{i} (°C)	230.1 (4.2) ^a	205.0 (2.5) ^b	198.4 (4.2) ^b	190.4 (3.0) ^b	230.7 (3.2) ^a
T_{m} (°C)	315.4 (3.0) ^a	314.4 (3.4) ^a	310.6 (0.6) ^a	315.6 (5.0) ^a	304.3 (1.7) ^b
T_{b} (°C)	525.7 (1.9) ^a	530.4 (1.5) ^b	584.4 (1.8) ^c	550.6 (2.2) ^d	560.0 (2.0) ^d
FR	0.24	0.44	0.25	0.19	0.17
$\text{CCI} \times 10^7$ (min ⁻² °C ⁻³)	8.0	9.2	9.5	8.3	8.1

^aAverage values with standard deviations (in parentheses). ^bMeans with a different superscript significantly differ ($p < 0.05$).

addition to those standards, some more information is needed to learn about the potential use of hydrochar as a biofuel. Ash agglomeration rates and the oxidation behavior of the fuel material in combustion are important issues in that respect. Regarding the first one, process water recycling is expected to raise fouling, slagging, and alkalinity due to the increased ash content of the resulting char (Table 1). Ash agglomeration rates changed after both conventional and PW-recycling HTC. After conventional HTC and the first PW-recycling run, the related indexes revealed a low risk of ash agglomeration ($R_{\text{b/a}}$: <1.0, SI and FI <0.6). However, in the second and third runs under recycled process water, the observed increase of those indexes is indicative of medium risk levels ($R_{\text{b/a}}$: >1.0, SI: >0.6). Although the AI index of all samples yielded intermediate values (>0.34), the resulting ashes could lead to glassy formations if not removed regularly.⁵⁴ Table S3 shows the mineral content of GPW and hydrochars. Monovalent metals are highly soluble under hydrothermal conditions, while divalent and trivalent ones increase their concentration in the solid phase.^{55,56} In this case, this trend is only observed in the HC from conventional HTC, while the hydrochars from PW-recycling runs show a gradual increase in metal content, including K. Despite the high solubility of K, probably saturation in the liquid fraction could promote the formation of salts that were retained in the solid phase. Figure S1 depicts metal and P contents in the process water. The concentration of the metal species gradually increased with PW recycling, reaching almost 15 g L⁻¹. K exhibited the highest concentration at 7.1 g L⁻¹, owing to its high solubility, followed by Ca at 5.4 g L⁻¹, which constitutes the major metallic component in the starting GPW.

The oxidation behavior of the hydrochars varied significantly throughout the HTC runs. Recycling of the process water reduced the T_{i} of the hydrochars from 205 °C in HC to 190 °C in HC2, which could be attributed to the higher VM content of the latter. T_{m} remained stable around 310 °C, where most of the oxidizable material decomposes. On the other

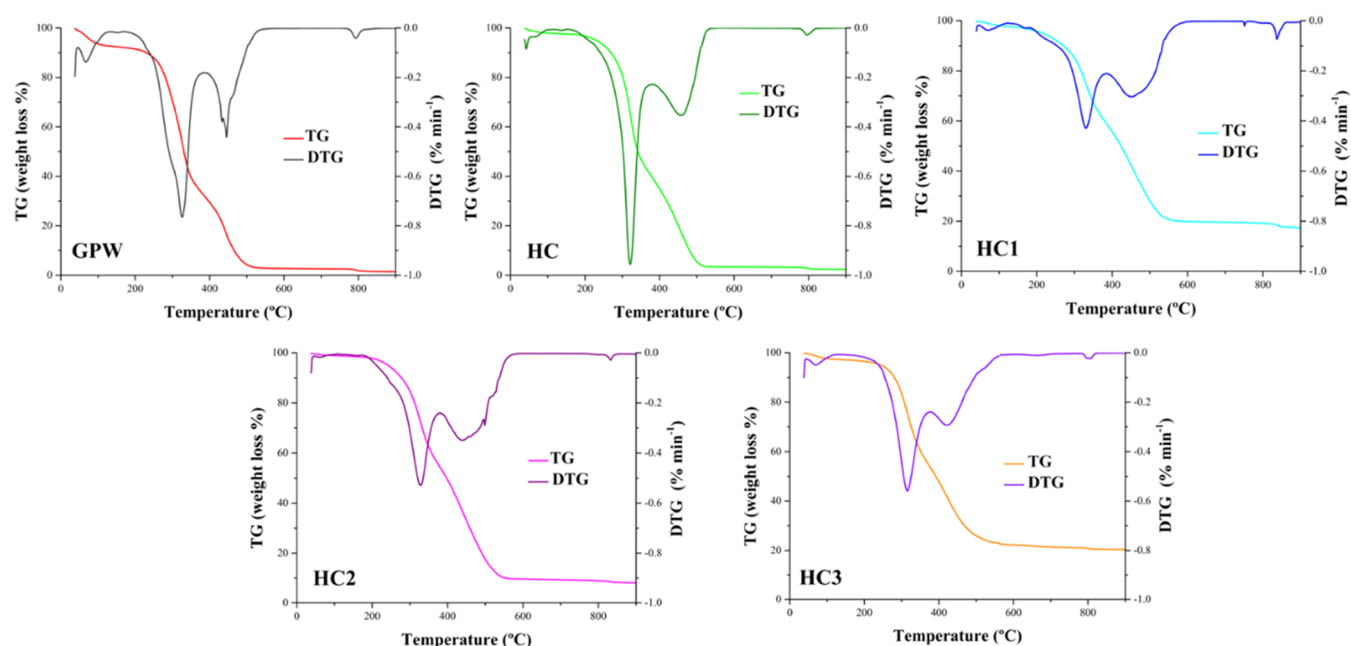


Figure 1. TG and DTG profiles of GPW and hydrochars.

hand, T_b showed an increasing trend up to 584 °C, indicating higher combustion efficiency and complete combustion of the hydrochars obtained by process water recycling. Sharma et al.²⁶ analyzed the cohydrothermal carbonization (co-HTC) of food waste and yard waste, reusing process water for up to 5 cycles. This revealed an enhanced reactivity of the hydrochar as the number of process water reuse cycles was increased, transitioning from an activation energy (E_a) of oxidation of 3 kJ mol⁻¹ in the first HTC cycle with fresh water to 2.5 kJ mol⁻¹ in the fifth cycle of process water recycling. The onset temperature (T_i) increased in the water cycle (T_i 320 °C) and then gradually decreased again to 304 °C. The mass yield increased by up to 6 percentage points, while the improvement in the higher heating value (HHV) was more moderate, ranging from 3 to 5%. Chen et al.¹⁹ also observed improved thermal stability of the hydrochars obtained by using recycled PW in the HTC of sweet potato waste. For biofuels, a high FC content is desirable because the components associated with that parameter commonly have high HHV and T_b , allowing improved combustion performance. In addition, FC regulates combustion stability, whereas high VM content can lead to rapid release of gases (including undesirable pollutants such as CO, VOCs, particulate matter, and NO_x), resulting in incomplete combustion and rapid consumption of solid biofuel.⁵⁷ The highest FR value was obtained for HC (0.44), due to the higher FC content (30 wt %), while in hydrochars obtained under process water recycling, these values gradually decreased consistently with the reduction of FC content. A higher FR value indicates better combustion stability and energetic efficiency.^{20,58} Arauzo et al.⁵⁰ and Ding et al.²⁰ observed a considerable increase in mass yield and energy recovery of up to 15 percentage points, along with a moderate increase in HHV of 6% in HTC with process water recycling of rice husk and spent grains (220 °C for 60 min). A decrease of the VM content and moderate increases of the FC and ash content were observed. This could suggest that HTC, at higher temperatures, exhibits a different behavior, avoiding the accumulation of VM in the hydrochar by transferring it to

the liquid fraction due to the high carbonization temperature, in contrast to the results observed in our study. Despite the increase in VM content, they apparently exhibit thermal behavior similar to the hydrochar obtained with DW. This, coupled with the moderate CCI values ($\sim 8.0 \times 10^{-7} \text{ min}^{-2} \text{ } ^\circ\text{C}^{-3}$) in hydrochars HC2 and HC3, indicates a reduced interest as biofuels. This highlights HC and HC1 as the most suitable for fuel application, meeting the criteria of ISO 17225-8 and showing better thermal stability according to thermogravimetric analysis. However, more in-depth study is needed to address other issues not analyzed in this work, such as gas emission analysis, particulate matter characterization, and experimental study of ash agglomeration, among others.^{59,60} In general, the recycling of process water led to an increase in VM and a lower FC content, causing a decrease in the onset temperature (T_i) up to 190 °C in HC2. This resulted in a more reactive but less thermally stable material. Furthermore, as mentioned, starting from the second cycle of process water recycling, the VM content exceeded 75%, limiting its suitability as a solid biofuel at the industrial level.

Figure 1 shows the thermogravimetric and derivative thermogravimetric profiles of hydrochars and the starting GPW in an air atmosphere. Quite similar DTG profiles can be observed, with a first high peak (250–320 °C) corresponding to VM and hemicellulose burnoff and a second peak (450–500 °C) ascribed to FC, cellulose, and lignin.⁶¹ However, hydrochars obtained upon process water recycling show a significant decrease in the intensity of the first and second peaks. This suggests a strong reduction or even almost complete absence of hemicellulose in those hydrochars. The small DTG peak in the temperature range of 770–800 °C can be attributed to carbonate decomposition.¹⁸

The morphology of the hydrochars and the starting GPW can be seen in the SEM micrographs of Figure S2. The raw fibrous structure of the GPW was basically respected in the hydrochars, given the moderate HTC temperature (180 °C). Some accumulation of spherical particles in the hydrochar structure can be observed, which could be due to the

Table 3. Main Characteristics of Process Water^{a,b}

	PW	PW1	PW2	PW3
Y_{PW} (%)	8.4 (0.4) ^a	13.0 (0.2) ^b	13.6 (0.3) ^b	19.4 (0.4) ^c
TS (g L ⁻¹)	42.2 (2.3) ^a	67.0 (6.1) ^b	69.6 (1.8) ^b	89.7 (0.7) ^c
VS (g L ⁻¹)	36.7 (2.9) ^a	53.6 (5.1) ^b	52.6 (1.4) ^b	69.2 (1.1) ^c
SCOD (g L ⁻¹)	57.5 (0.6) ^a	89.3 (2.3) ^b	95.8 (0.7) ^c	96.7 (1.6) ^c
TOC (g L ⁻¹)	26.0 (0.9) ^a	40.1 (1.6) ^b	49.8 (1.0) ^c	53.7 (0.0) ^d
TVFA (g acetic acid L ⁻¹)	4.2 (0.4) ^a	7.2 (0.2) ^b	12.0 (0.7) ^c	20.3 (0.1) ^d
TKN (g L ⁻¹)	1.1 (0.1) ^a	3.3 (0.1) ^b	3.9 (0.0) ^c	5.1 (0.1) ^d
NH ₃ -N (g L ⁻¹)	0.2 (0.0) ^a	0.2 (0.0) ^a	0.3 (0.0) ^b	0.4 (0.1) ^b
Org-N (g L ⁻¹)	1.0 (0.1) ^a	3.1 (0.1) ^b	3.6 (0.1) ^c	4.7 (0.1) ^d
pH	3.9 (0.1) ^a	3.9 (0.1) ^a	3.9 (0.0) ^a	3.8 (0.1) ^a
conductivity (mS cm ⁻¹)	7.9 (0.8) ^a	13.7 (1.5) ^b	18.7 (0.2) ^c	24.3 (0.2) ^d

^aAverage values with standard deviations (in parentheses). ^bMeans with a different superscript significantly differ ($p < 0.05$).

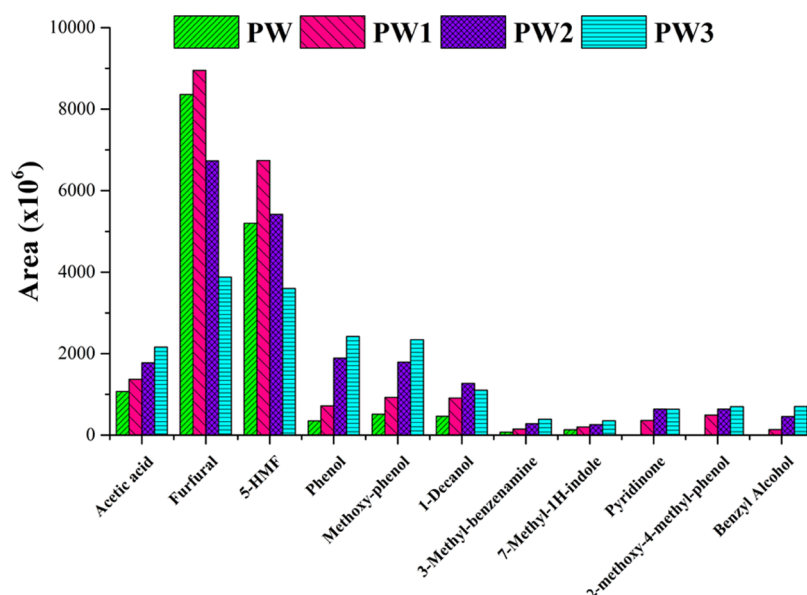


Figure 2. Chemical species in process water determined by CG-MS.

accumulation of material ascribed to VM by the formation of secondary hydrochar. On the other hand, the analysis of energy-dispersive X-ray spectroscopy (EDX) indicated that significant regions of the solids correspond to Ca, K, and Si species. Arauzo et al.⁵⁰ observed that the HTC temperature has a high effect on the change of hydrochar morphology upon successive PW recycling. Similar results were described by Ding et al.,²⁰ who observed that HTC of rice husk at 220 °C partially destroyed the fibrous structure of the lignocellulosic biomass, leading to a growing accumulation of small particles on the surface of the hydrochar as the number of reuse cycles of PW increased. FTIR analysis of the hydrochar surface is depicted in Figure S3. Examination of the FTIR spectra for HC and HC3 revealed some not very significant variations in the surface functional groups. A reduction in vibrations was observed around 3400–3485 cm⁻¹, corresponding to the formation of the O–H bonds. Lang et al.⁶² highlighted that the main bonds affected after CaO-assisted HTC of swine manure at 180–220 °C were O–H bonds (3340 cm⁻¹), as well as ketone and carboxylic groups at 1645 and 1540 cm⁻¹, respectively. This indicates a high degree of dehydration and decarboxylation of the starting biomass. They also observed a moderate shift in the vibrations of the 1600 cm⁻¹ band corresponding to aromatic species. Zhuang et al.⁶³ studied the

change in the functional groups of lignocellulosic biomasses at different reaction temperatures, observing that the O-containing functional groups weaken with increasing temperature (>200 °C), while the C–C and C=C groups strengthen and vibrating more intensely, showing an improvement of the surface layer structure of hydrochars. In summary, the overall process indicates that water recirculation has a negligible influence on changing the functional groups of the hydrochar structure (Figure S2), especially when compared to factors such as temperature⁶² or catalyst.⁶³ TPD spectra (Figure S4 and Table S3) allow assessment of functional groups on the hydrochar surface. CO₂ evolved in TPD is commonly ascribed to carboxylic groups, lactones, and anhydrides, while CO is mostly associated with phenolic groups, carbonyls, and ethers.⁶⁴ The hydrochars obtained under PW recycling released significantly less CO₂ (Table S3), suggesting a lower presence of carboxylic groups on their surface, consistent with deep breakdown of hemicellulose (see Table 1). In addition, the TPD of the HC hydrochar (conventional HTC) showed the lowest CO/CO₂ ratio (0.28), suggesting a higher concentration of organic components prone to complete combustion.⁶⁵ That ratio is lower than the one of GPW (0.33), and a monotonically significant increase is observed for the HC1, HC2, and HC3 hydrochars, probably ascribed to a

decreasing presence of carboxylic surface groups and a growing of aromatic or cyclic species from secondary HTC reactions (polymerization, condensation, and Maillard reactions, as mentioned before). This is consistent with the higher temperatures for complete combustion observed in the thermogravimetric profiles.

3.2. Effect of Process Water Recycling on the Composition of the Liquid Phase from HTC. Table 3 shows the main characteristics of the liquid phase after the HTC runs and the yield values for that fraction (Y_{PW}). Those values increased significantly with PW recycling from 8.4 wt % in conventional HTC to 19.4 wt % in PW3, accompanied, as expected, by a gradual increase of TS, VS, SCOD, and TOC, as well as TVFA. The VS/TS ratio decreased from 0.87 in PW to 0.77 in PW3, suggesting that the process water is not only enriched in soluble organic matter but also accumulates inorganic components such as metal ions at a higher rate. Organic matter content showed a significant increase in the successive PW-recycling runs, with TOC doubling from PW to PW3 and somewhat less in the case of COD (1.75-fold). With respect to the inorganic matter, a significant increase of salinity was evidenced by the evolution of conductivity (3-fold), reaching 24 mS cm^{-1} in PW3. A similar trend was observed with VFAs, which increased their concentration in PW3 up to almost 5-fold with respect to PW. VFA analyses (Figure S5) showed a gradual increase in all individual VFAs, with acetic acid (C2) being the prevailing one (80–85%), growing from 3.2 g L^{-1} in PW to 18.7 g L^{-1} in PW3. TKN showed a similar trend to organic matter, reaching almost a 5-fold increase between PW and PW3, with no significant variation in $\text{NH}_3\text{-N}$ (~ 0.2 to 0.4 g L^{-1}). The low carbonization temperature (180°C) allows for transferring only organic N species to the process water, without nitrogen mineralization,⁴² so that Org-N (proteins and amino acids) reached $\sim 92\%$ of the TKN in the process water. The pH of the process water was always acidic.

The evolution and diversity of organic compounds in the process water were analyzed by GC/MS (Figure 2). The high presence of furfural and 5-HMF in PW1 is remarkable and probably attributed to the fact that some organic compounds in the process water may promote dehydration reactions of sugars, derived mainly from the hydrolysis of hemicellulose and, to a lesser extent, cellulose. However, as the process water was reused in successive cycles, these compounds gradually decreased, indicating that they might have been transferred to the solid fraction as secondary hydrochar or converted into intermediate species.^{48,66} On the other hand, aromatic compounds, such as phenol and methoxyphenol, showed a gradual increase, possibly due to the partial hydrolysis of lignin.^{22,67} Köchermann et al.⁴² observed an increase of 5-HMF and phenol up to four PW-recycling runs in municipal green waste HTC, and Wang et al.⁶⁸ observed a similar increase of furfural and 5-HMF in laminaria HTC.

Figure 3 shows the C distribution in the hydrochar, process water, and gas phase (by difference). Although Y_{HC} and the C content of the hydrochar increase with PW recycling, the C balance showed a lower C retention in the hydrochar (from 79% in HC to 66% in HC3). The increase in C migrated to the liquid fraction can be ascribed to GPW hydrolysis reactions occurring at a faster rate than side reactions involved in secondary hydrochar formation,⁷ and the VFAs formed do not participate in the latter, unlike aromatic compounds and nitrogen-containing aromatic compounds.⁶⁸

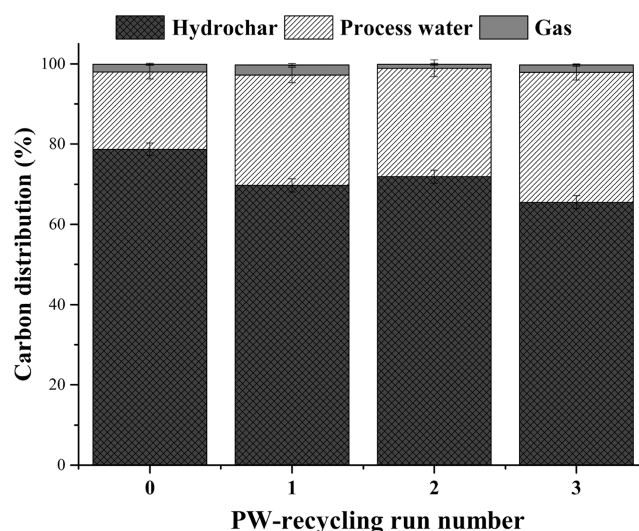


Figure 3. Carbon (C) distribution in hydrochar, process water, and gas phase after HTC runs.

3.3. Anaerobic Digestion of Process Water. Figure 4 shows methane production and organic matter removal after the AD of process waters. The highest methane production was achieved with PW and PW1 (295 and $302 \text{ N mL CH}_4 \text{ g}^{-1} \text{ COD}_{\text{added}}$, respectively), decreasing significantly with the process waters obtained from the second recycling run. Consistent with methane production, organic matter removal decreased significantly from the second cycle, even though these process waters (PW2 and PW3) showed a high TVFA content (see Table 3 and Figure S5), compounds easily assimilated by methanogenic archaea. The lower methane production could be attributed to the presence of hard-to-degrade compounds such as N-containing aromatic species²⁹ (see Figure 2). In the AD of process water from HTC of food and yard wastes, methane production reached $220 \text{ mL CH}_4 \text{ g}^{-1} \text{ COD}_{\text{added}}$, and COD removal was around 52% (SCOD) after the first PW reuse cycle²⁶ even though the process water came from a highly biodegradable substrate. This could be attributed to the high carbonization temperature (220°C), which promoted the formation of refractory compounds that are difficult to degrade by anaerobic treatment.

Figure 5 shows the total energy recovery in hydrochar from HTC plus methane in the biogas from subsequent AD of the process water. The hydrochar represents by far most of that energy recovery, but biogas also makes a significant additional contribution. PW recycling improves energy recovery but with a decreasing significance after successive cycles. However, the quality of the biofuel obtained must be considered since, as discussed before, the hydrochars from the second and following PW-recycling runs were enriched in VM, exceeding the limit established by ISO 17225-8³⁰ standard (75 wt %). With a single recycling, the total energy recovery reached 96% (90% hydrochar plus 6% methane). This approach yielded a hydrochar with adequate combustion characteristics and a process water with both high anaerobic biodegradability (66%) and methane production ($302 \text{ N mL CH}_4 \text{ g}^{-1} \text{ COD}_{\text{added}}$).

4. CONCLUSIONS

Hydrothermal carbonization allows for sustainable energy recovery from biomass wastes of low energetic density. The main product of the process is a biochar, so-called hydrochar,

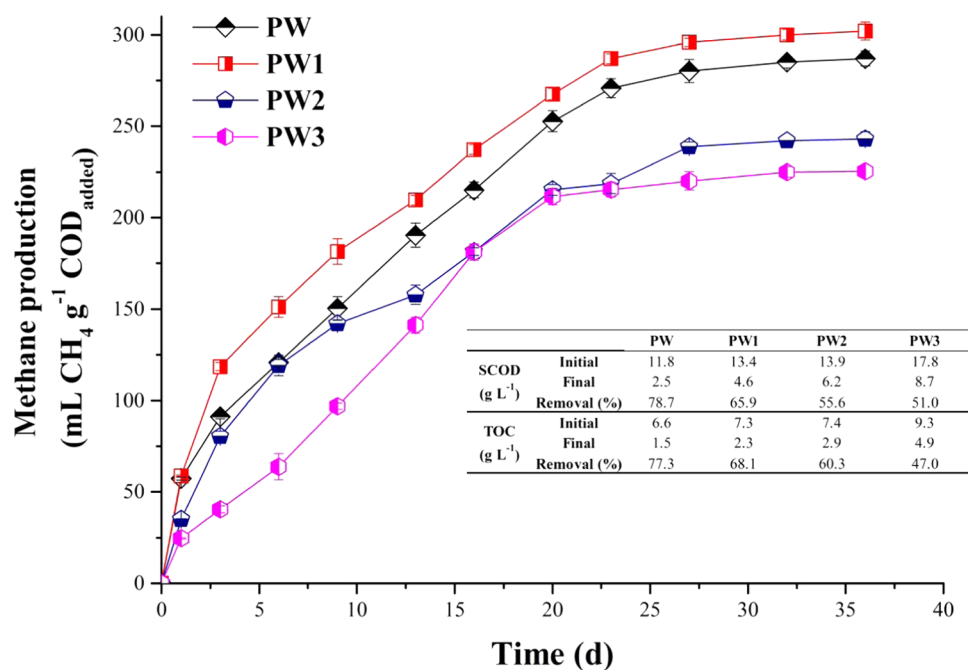


Figure 4. Methane production and organic matter removal from the anaerobic digestion of process water.

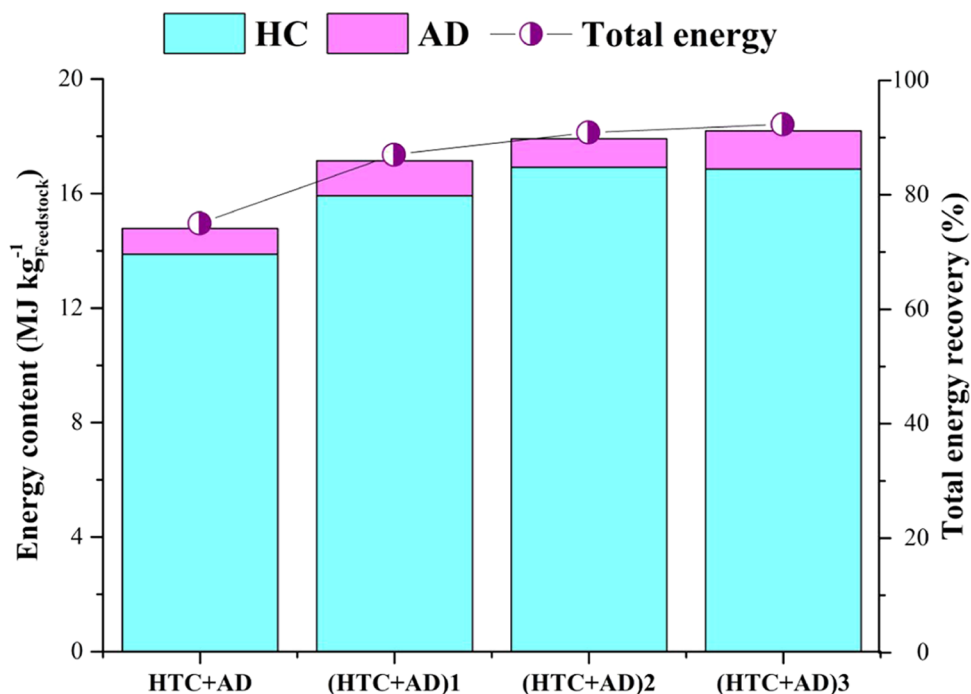


Figure 5. Total energy recovery from hydrochar (HTC) and methane (AD).

more or less useful as a solid fuel depending on its combustion-related properties. However, a liquid fraction is also produced, representing a high-organic-load secondary waste, so-called process water, which requires effective management. Process water recycling emerges as a potential solution in that respect, allowing improvement of the quality of the hydrochar and increase of the energy yield of the HTC process, as demonstrated in the current work using garden and park waste, representative biomass residue of lignocellulosic constitution. The resulting hydrochar showed a higher reactivity and combustion temperature and a lower chance of

ash sintering. A single recycling of process water appears to be the optimal solution, allowing a significant improvement in the energy yield compared to conventional HTC. After subsequent cycles, the hydrochars showed an increase in volatile matter content, exceeding the limit specified in the ISO standard for industrial use as solid biofuel as well as higher ash and N content. This can be attributed to the growing formation of secondary hydrochar. Concurrently, the organic and inorganic matter contents of the process water increased upon repeated recycling. Anaerobic digestion of the process water allowed high methane production and organic matter removal,

especially with the process water resulting from the first recycling run. That represents an additional contribution to energy recovery while significantly reducing the polluting organic load (COD and TOC) of the final liquid waste. Total energy recovery gradually increased with process water recycling but at a very small rate in the successive runs following the first recycling, supporting the above conclusion that single recycling is the optimal approach.

■ ASSOCIATED CONTENT

SI Supporting Information

The Supporting Information is available free of charge at <https://pubs.acs.org/doi/10.1021/acssuschemeng.3c08438>.

Fouling and slagging indexes. Main mineral species in feedstock and hydrochars. CO and CO₂ released by temperature-programmed desorption from feedstock and hydrochars. Metal and P concentration in the process water, SEM images, FTIR, and TPD spectra of hydrochars, VFA concentration in the process water. (PDF)

■ AUTHOR INFORMATION

Corresponding Authors

Juan J. Rodríguez – Chemical Engineering Department, Universidad Autónoma de Madrid, 28049 Madrid, Spain; orcid.org/0000-0002-3497-9929; Email: juanjo.rodriguez@uam.es

Angel F. Mohedano – Chemical Engineering Department, Universidad Autónoma de Madrid, 28049 Madrid, Spain; Email: angelf.mohedano@uam.es

Authors

Ricardo Paul Ipiales – Chemical Engineering Department, Universidad Autónoma de Madrid, 28049 Madrid, Spain; Arquimea-Agrotech, 28400 Madrid, Spain

Diana Pimentel-Betancurt – Chemical Engineering Department, Universidad Autónoma de Madrid, 28049 Madrid, Spain; Molecular Biology Department, FCEFQyN, Universidad Nacional de Río Cuarto, 5800 Córdoba, Argentina; orcid.org/0000-0001-6397-2497

Elena Diaz – Chemical Engineering Department, Universidad Autónoma de Madrid, 28049 Madrid, Spain; orcid.org/0000-0003-1020-6240

Angeles de la Rubia – Chemical Engineering Department, Universidad Autónoma de Madrid, 28049 Madrid, Spain

Complete contact information is available at:

<https://pubs.acs.org/doi/10.1021/acssuschemeng.3c08438>

Author Contributions

R.P.I.: investigation, formal analysis, and writing—original draft. D.P.-B.: investigation, formal analysis, and writing—original draft. E.D.: funding acquisition, writing—review and editing, and supervision. A.d.l.R.: conceptualization, formal analysis, funding acquisition, methodology, resources, writing—review and editing, and supervision. A.F.M.: conceptualization, funding acquisition, methodology, resources, writing—review and editing, supervision, and project administration. J.J.R.: conceptualization, funding acquisition, methodology, resources, writing—review and editing, supervision, and project administration.

Notes

The authors declare no competing financial interest.

■ ACKNOWLEDGMENTS

The authors greatly appreciate funding from Spanish MCIN/AEI/10.13039/501100011033 and European Union “NextGenerationEU/PRTR” (TED2021-130287B-I00, PDC2021-120755-I00, and PID2022-138632OB-I00). R.P.I. acknowledges the financial support from the Community of Madrid (IND2019/AMB-17092) and Arquimea Agrotech Company.

■ ABBREVIATIONS

R_{b/a}: acid base ratio; AI: alkali index; AD: anaerobic digestion; T_b: burnout temperature; COD: chemical oxygen demand; CCI: comprehensive combustibility index; DTG: derivative thermogravimetry; DW: deionized water; EDX: energy-dispersive X-ray spectroscopy; E_{yield}: energy yield; FC: fixed carbon; FI: fouling index; FTIR: Fourier transform infrared spectroscopy; FR: fuel ratio; GPW: garden and park waste; HHV: higher heating value; Y_{HC}: hydrochar mass yield; HTC: hydrothermal carbonization; T_i: ignition temperature; ISR: inoculum–substrate ratio; T_m: maximum loss weight temperature; PW: process water; Y_{PW}: process water yield; SEM: scanning electron microscopy; SI: slagging index; SCOD: soluble chemical oxygen demand; SMP: specific methane production; TG: thermogravimetric; TOC: total organic carbon; TKN: total Kjeldahl nitrogen; TS: total solids; VFA: volatile fatty acid; VM: volatile matter

■ REFERENCES

- (1) Khosravi, A.; Zheng, H.; Liu, Q.; Hashemi, M.; Tang, Y.; Xing, B. Production and Characterization of Hydrochars and Their Application in Soil Improvement and Environmental Remediation. *Chem. Eng. J.* **2022**, *430*, No. 133142.
- (2) Ipiales, R. P.; Mohedano, A. F.; Diaz-portuondo, E.; Diaz, E.; de la Rubia, M. A. Co-Hydrothermal Carbonization of Swine Manure and Lignocellulosic Waste: A New Strategy for the Integral Valorization of Biomass Wastes. *Waste Manage.* **2023**, *169*, 267–275.
- (3) Suarez, E.; Tobajas, M.; Mohedano, A. F.; Reguera, M.; Esteban, E.; de la Rubia, A. Effect of Garden and Park Waste Hydrochar and Biochar in Soil Application: A Comparative Study. *Biomass Convers. Biorefin.* **2023**, *13*, 16479–16493, DOI: [10.1007/s13399-023-04015-0](https://doi.org/10.1007/s13399-023-04015-0).
- (4) Lu, X.; Jordan, B.; Berge, N. D. Thermal Conversion of Municipal Solid Waste via Hydrothermal Carbonization: Comparison of Carbonization Products to Products from Current Waste Management Techniques. *Waste Manage.* **2012**, *32* (7), 1353–1365.
- (5) Diaz, E.; Manzano, F. J.; Villamil, J.; Rodriguez, J. J.; Mohedano, A. F. Low-Cost Activated Grape Seed-Derived Hydrochar through Hydrothermal Carbonization and Chemical Activation for Sulfamethoxazole Adsorption. *Appl. Sci.* **2019**, *9*, 5127.
- (6) Lucian, M.; Volpe, M.; Gao, L.; Piro, G.; Goldfarb, J. L.; Fiori, L. Impact of Hydrothermal Carbonization Conditions on the Formation of Hydrochars and Secondary Chars from the Organic Fraction of Municipal Solid Waste. *Fuel* **2018**, *233*, 257–268.
- (7) Yang, G.; Liu, H.; Li, Y.; Zhou, Q.; Jin, M.; Xiao, H.; Yao, H. Kinetics of Hydrothermal Carbonization of Kitchen Waste Based on Multi-Component Reaction Mechanism. *Fuel* **2022**, *324*, No. 124693.
- (8) Pecchi, M.; Baratieri, M.; Goldfarb, J. L.; Maag, A. R. Effect of Solvent and Feedstock Selection on Primary and Secondary Chars Produced via Hydrothermal Carbonization of Food Wastes. *Bioresour. Technol.* **2022**, *348*, No. 126799.
- (9) Wang, Q.; Sun, S.; Wu, C.; Sun, B. Kinetic Study on Flue Gas Torrefaction of Real Components of Corn Stalk. *Thermochim. Acta* **2023**, *719*, No. 179406.
- (10) Wu, S.; Wang, Q.; Wu, D.; Cui, D.; Wu, C.; Bai, J.; Xu, F.; Liu, B.; Shan, Z.; Zhang, J. Influence of Temperature and Process Water Circulation on Hydrothermal Carbonization of Food Waste for Sustainable Fuel Production. *J. Energy Inst.* **2024**, *112*, No. 101459.

- (11) Ipiates, R. P.; de la Rubia, M. A.; Diaz, E.; Mohedano, A. F.; Rodriguez, J. J. Integration of Hydrothermal Carbonization and Anaerobic Digestion for Energy Recovery of Biomass Waste: An Overview. *Energy Fuels* **2021**, *35*, 17032–17050.
- (12) Heidari, M.; Dutta, A.; Acharya, B.; Mahmud, S. A Review of the Current Knowledge and Challenges of Hydrothermal Carbonization for Biomass Conversion. *J. Energy Inst.* **2019**, *92*, 1779–1799.
- (13) Stutzenstein, P.; Weiner, B.; Köhler, R.; Pfeifer, C.; Kopinke, F. D. Wet Oxidation of Process Water from Hydrothermal Carbonization of Biomass with Nitrate as Oxidant. *Chem. Eng. J.* **2018**, *339*, 1–6.
- (14) Weide, T.; Brüggling, E.; Wetter, C. Anaerobic and Aerobic Degradation of Wastewater from Hydrothermal Carbonization (HTC) in a Continuous, Three-Stage and Semi-Industrial System. *J. Environ. Chem. Eng.* **2019**, *7*, No. 102912.
- (15) Langone, M.; Sabia, G.; Petta, L.; Zanetti, L.; Leoni, P.; Basso, D. Evaluation of the Aerobic Biodegradability of Process Water Produced by Hydrothermal Carbonization and Inhibition Effects on the Heterotrophic Biomass of an Activated Sludge System. *J. Environ. Manage.* **2021**, *299*, No. 113561.
- (16) Gaur, R. Z.; Khoury, O.; Zohar, M.; Poverenov, E.; Darzi, R.; Laor, Y.; Posmanik, R. Hydrothermal Carbonization of Sewage Sludge Coupled with Anaerobic Digestion: Integrated Approach for Sludge Management and Energy Recycling. *Energy Convers. Manage.* **2020**, *224*, No. 113353.
- (17) Blach, T.; Lechevallier, P.; Engelhart, M. Effect of Temperature during the Hydrothermal Carbonization of Sewage Sludge on the Aerobic Treatment of the Produced Process Waters. *J. Water Process Eng.* **2023**, *51*, No. 103368.
- (18) Ipiates, R. P.; Mohedano, A. F.; Diaz, E.; de la Rubia, M. A. Energy Recovery from Garden and Park Waste by Hydrothermal Carbonisation and Anaerobic Digestion. *Waste Manage.* **2022**, *140*, 100–109.
- (19) Chen, X.; Ma, X.; Peng, X.; Lin, Y.; Wang, J.; Zheng, C. Effects of Aqueous Phase Recirculation in Hydrothermal Carbonization of Sweet Potato Waste. *Bioresour. Technol.* **2018**, *267* (381), 167–174.
- (20) Ding, Y.; Guo, C.; Qin, S.; Wang, B.; Zhao, P.; Cui, X. Effects of Process Water Recirculation on Yields and Quality of Hydrochar from Hydrothermal Carbonization Process of Rice Husk. *J. Anal. Appl. Pyrolysis* **2022**, *166*, No. 105618.
- (21) Mau, V.; Neumann, J.; Wehrli, B.; Gross, A. Nutrient Behavior in Hydrothermal Carbonization Aqueous Phase Following Recirculation and Reuse. *Environ. Sci. Technol.* **2019**, *53*, 10426–10434.
- (22) Boutaieb, M.; Román, S.; Ledesma, B.; Sabio, E.; Guiza, M.; Ouederni, A. Towards a More Efficient Hydrothermal Carbonization: Processing Water Recirculation under Different Conditions. *Waste Manage.* **2021**, *132*, 115–123.
- (23) Stemann, J.; Putschew, A.; Ziegler, F. Hydrothermal Carbonization: Process Water Characterization and Effects of Water Recirculation. *Bioresour. Technol.* **2013**, *143*, 139–146.
- (24) Wang, R.; Jin, Q.; Ye, X.; Lei, H.; Jia, J.; Zhao, Z. Effect of Process Wastewater Recycling on the Chemical Evolution and Formation Mechanism of Hydrochar from Herbaceous Biomass during Hydrothermal Carbonization. *J. Cleaner Prod.* **2020**, *277*, No. 123281.
- (25) Harisankar, S.; Francis Prashanth, P.; Nallasivam, J.; Vishnu Mohan, R.; Vinu, R. Effects of Aqueous Phase Recirculation on Product Yields and Quality from Hydrothermal Liquefaction of Rice Straw. *Bioresour. Technol.* **2021**, *342*, No. 125951.
- (26) Sharma, H. B.; Panigrahi, S.; Vanapalli, K. R.; Cheela, V. R. S.; Venna, S.; Dubey, B. Study on the Process Wastewater Reuse and Valorisation during Hydrothermal Co-Carbonization of Food and Yard Waste. *Sci. Total Environ.* **2022**, *806*, 150748.
- (27) Ipiates, R. P.; Sarrion, A.; Diaz, E.; Diaz-Portuondo, E.; Mohedano, A. F.; de la Rubia, A. Strategies to Improve Swine Manure Hydrochar: HCl-Assisted Hydrothermal Carbonization versus Hydrochar Washing. *Biomass Convers. Biorefin.* **2023**, *13*, 16467–16478.
- (28) Zhao, P.; Lin, C.; Li, Y.; Zhang, J.; Huang, N.; Cui, X.; Liu, F.; Guo, Q. Combustion and Slagging Characteristics of Hydrochar Derived from the Co-Hydrothermal Carbonization of PVC and Alkali Coal. *Energy* **2022**, *244*, No. 122653.
- (29) Marin-Batista, J. D.; Villamil, J. A.; Rodriguez, J. J.; Mohedano, A. F.; de la Rubia, M. A. Valorization of Microalgal Biomass by Hydrothermal Carbonization and Anaerobic Digestion. *Bioresour. Technol.* **2019**, *274*, 395–402.
- (30) International Organization for Standardization ISO/TS 17225-8. Solid Biofuels – Fuel Specifications and Classes. Graded Thermally Treated and Densified Biomass Fuels, 2016.
- (31) *Standard Test Methods for Proximate Analysis of Coal and Coke by Macro Thermogravimetric Analysis. Method D7582-15* ASTM International: PA; 2015.
- (32) Suarez, E.; Tobajas, M.; Mohedano, A. F.; de la Rubia, M. A. Energy Recovery from Food Waste and Garden and Park Waste: Anaerobic Co-Digestion versus Hydrothermal Treatment and Anaerobic Co-Digestion. *Chemosphere* **2022**, *297*, No. 134223.
- (33) Zhang, D.; Han, P.; Yang, R.; Wang, H.; Lin, W.; Zhou, W.; Yan, Z.; Qi, Z. Fuel Properties and Combustion Behaviors of Fast Torrefied Pinewood in a Heavily Loaded Fixed-Bed Reactor by Superheated Steam. *Bioresour. Technol.* **2021**, *342*, No. 125929.
- (34) Masiá, A. T.; Buhre, B. J. P.; Gupta, R. P.; Wall, T. F. Characterising Ash of Biomass and Waste. *Fuel Process. Technol.* **2007**, *88*, 1071–1081.
- (35) Cao, Z.; Hülsemann, B.; Wüst, D.; Oechsner, H.; Lautenbach, A.; Kruse, A. Effect of Residence Time during Hydrothermal Carbonization of Biogas Digestate on the Combustion Characteristics of Hydrochar and the Biogas Production of Process Water. *Bioresour. Technol.* **2021**, *333*, No. 125110.
- (36) *Standard Methods for the Examination of Water and Wastewater*, 21st ed.; American Public Health Association: Washington, DC, 2005.
- (37) de la Rubia, M. A.; Villamil, J. A.; Rodriguez, J. J.; Mohedano, A. F. Effect of Inoculum Source and Initial Concentration on the Anaerobic Digestion of the Liquid Fraction from Hydrothermal Carbonisation of Sewage Sludge. *Renewable Energy* **2018**, *127*, 697–704.
- (38) de la Rubia, M. A.; Villamil, J. A.; Rodriguez, J. J.; Borja, R.; Mohedano, A. F. Mesophilic Anaerobic Co-Digestion of the Organic Fraction of Municipal Solid Waste with the Liquid Fraction from Hydrothermal Carbonization of Sewage Sludge. *Waste Manage.* **2018**, *76*, 315–322.
- (39) Villamil, J. A.; Mohedano, A. F.; Rodriguez, J. J.; de la Rubia, M. A. Valorisation of the Liquid Fraction from Hydrothermal Carbonisation of Sewage Sludge by Anaerobic Digestion. *J. Chem. Technol. Biotechnol.* **2018**, *93*, 450–456.
- (40) Taskin, E.; de Castro Bueno, C.; Allegretta, I.; Terzano, R.; Rosa, A. H.; Loffredo, E. Multianalytical Characterization of Biochar and Hydrochar Produced from Waste Biomasses for Environmental and Agricultural Applications. *Chemosphere* **2019**, *233*, 422–430.
- (41) Picone, A.; Volpe, M.; Codignole Lùz, F.; Malik, W.; Volpe, R.; Messineo, A. Co-Hydrothermal Carbonization with Process Water Recirculation as a Valuable Strategy to Enhance Hydrochar Recovery with High Energy Efficiency. *Waste Manage.* **2024**, *175*, 101–109.
- (42) Köchermann, J.; Görsch, K.; Wirth, B.; Mühlenberg, J.; Klemm, M. Hydrothermal Carbonization: Temperature Influence on Hydrochar and Aqueous Phase Composition during Process Water Recirculation. *J. Environ. Chem. Eng.* **2018**, *6* (4), 5481–5487.
- (43) Cao, X.; Ro, K. S.; Chappell, M.; Li, Y.; Mao, J. Chemical Structures of Swine-Manure Chars Produced under Different Carbonization Conditions Investigated by Advanced Solid-State ¹³C Nuclear Magnetic Resonance (NMR) Spectroscopy. *Energy Fuels* **2011**, *25* (1), 388–397.
- (44) Funke, A.; Ziegler, F. Hydrothermal Carbonization of Biomass: A Summary and Discussion of Chemical Mechanisms for Process Engineering. *Biofuels Bioprod. Biorefin.* **2010**, *4* (2), 160–177.
- (45) Volpe, M.; Messineo, A.; Mäkelä, M.; Barr, M. R.; Volpe, R.; Corrado, C.; Fiori, L. Reactivity of Cellulose during Hydrothermal Carbonization of Lignocellulosic Biomass. *Fuel Process. Technol.* **2020**, *206*, No. 106456.

- (46) Lavoie, J.-M.; Baré, W.; Bilodeau, M. Depolymerization of Steam-Treated Lignin for the Production of Green Chemicals. *Bioresour. Technol.* **2011**, *102* (7), 4917–4920.
- (47) Wang, Z.; Huang, J.; Wang, B.; Hu, W.; Xie, D.; Liu, S.; Qiao, Y. Co-Hydrothermal Carbonization of Sewage Sludge and Model Compounds of Food Waste: Influence of Mutual Interaction on Nitrogen Transformation. *Sci. Total Environ.* **2022**, *807*, 150997.
- (48) Leng, S.; Li, W.; Han, C.; Chen, L.; Chen, J.; Fan, L.; Lu, Q.; Li, J.; Leng, L.; Zhou, W. Aqueous Phase Recirculation during Hydrothermal Carbonization of Microalgae and Soybean Straw: A Comparison Study. *Bioresour. Technol.* **2020**, *298*, No. 122502.
- (49) Sarrion, A.; de la Rubia, A.; Coronella, C.; Mohedano, A. F.; Diaz, E. Acid-Mediated Hydrothermal Treatment of Sewage Sludge for Nutrient Recovery. *Sci. Total Environ.* **2022**, *838*, No. 156494, DOI: 10.1016/j.scitotenv.2022.156494.
- (50) Arauzo, P. J.; Olszewski, M. P.; Wang, X.; Pfersich, J.; Sebastian, V.; Manyà, J.; Hedín, N.; Kruse, A. Assessment of the Effects of Process Water Recirculation on the Surface Chemistry and Morphology of Hydrochar. *Renewable Energy* **2020**, *155*, 1173–1180.
- (51) He, C.; Zhang, Z.; Ge, C.; Liu, W.; Tang, Y.; Zhuang, X.; Qiu, R. Synergistic Effect of Hydrothermal Co-Carbonization of Sewage Sludge with Fruit and Agricultural Wastes on Hydrochar Fuel Quality and Combustion Behavior. *Waste Manage.* **2019**, *100*, 171–181.
- (52) Lee, J.; Lee, K.; Sohn, D.; Kim, Y. M.; Park, K. Y. Hydrothermal Carbonization of Lipid Extracted Algae for Hydrochar Production and Feasibility of Using Hydrochar as a Solid Fuel. *Energy* **2018**, *153*, 913–920.
- (53) Picone, A.; Volpe, M.; Messineo, A. Process Water Recirculation during Hydrothermal Carbonization of Waste Biomass: Current Knowledge and Challenges. *Energies* **2021**, *14*, 2962.
- (54) Mäkelä, M.; Fullana, A.; Yoshikawa, K. Ash Behavior during Hydrothermal Treatment for Solid Fuel Applications. Part 1: Overview of Different Feedstock. *Energy Convers. Manage.* **2016**, *121*, 402–408.
- (55) Alhnidi, M. J.; Wüst, D.; Funke, A.; Hang, L.; Kruse, A. Fate of Nitrogen, Phosphate, and Potassium during Hydrothermal Carbonization and the Potential for Nutrient Recovery. *ACS Sustainable Chem. Eng.* **2020**, *8*, 15507–15516.
- (56) Sarrion, A.; Ipiales, R. P.; de la Rubia, M. A.; Mohedano, A. F.; Diaz, E. Chicken Meat and Bone Meal Valorization by Hydrothermal Treatment and Anaerobic Digestion: Biofuel Production and Nutrient Recovery. *Renewable Energy* **2023**, *204*, 652–660.
- (57) Lang, Q.; Liu, Z.; Li, Y.; Xu, J.; Li, J.; Liu, B.; Sun, Q. Combustion Characteristics, Kinetic and Thermodynamic Analyses of Hydrochars Derived from Hydrothermal Carbonization of Cattle Manure. *J. Environ. Chem. Eng.* **2022**, *10* (1), No. 106938.
- (58) Aliyu, M.; Iwabuchi, K.; Itoh, T. Upgrading the Fuel Properties of Hydrochar by Co-Hydrothermal Carbonisation of Dairy Manure and Japanese Larch (*Larix Kaempferi*): Product Characterisation, Thermal Behaviour, Kinetics and Thermodynamic Properties. *Biomass Convers. Biorefin.* **2021**, *13*, 11917–11932, DOI: 10.1007/s13399-021-02045-0.
- (59) Magdziarz, A.; Gajek, M.; Nowak-Woźny, D.; Wilk, M. Mineral Phase Transformation of Biomass Ashes—Experimental and Thermodynamic Calculations. *Renewable Energy* **2018**, *128*, 446–459.
- (60) Niu, Y.; Tan, H.; Ma, L.; Pourkashanian, M.; Liu, Z.; Liu, Y.; Wang, X.; Liu, H.; Xu, T. Slagging Characteristics on the Superheaters of a 12 MW Biomass-Fired Boiler. *Energy Fuels* **2010**, *24*, S222–S227.
- (61) Bardhan, M.; Novera, T. M.; Tabassum, M.; Islam, M. A.; Islam, M. A.; Hameed, B. H. Co-Hydrothermal Carbonization of Different Feedstocks to Hydrochar as Potential Energy for the Future World: A Review. *J. Cleaner Prod.* **2021**, *298*, No. 126734.
- (62) Lang, Q.; Zhang, B.; Liu, Z.; Jiao, W.; Xia, Y.; Chen, Z.; Li, D.; Ma, J.; Gai, C. Properties of Hydrochars Derived from Swine Manure by CaO Assisted Hydrothermal Carbonization. *J. Environ. Manage.* **2019**, *233*, 440–446.
- (63) Zhuang, X.; Zhan, H.; Song, Y.; He, C.; Huang, Y.; Yin, X.; Wu, C. Insights into the Evolution of Chemical Structures in Lignocellulose and Non-Lignocellulose Biowastes during Hydrothermal Carbonization (HTC). *Fuel* **2019**, *236*, 960–974.
- (64) Figueiredo, J. L.; Pereira, M. F. R.; Freitas, M. M. A.; Órfão, J. J. M. Modification of the Surface Chemistry of Activated Carbons. *Carbon* **1999**, *37* (9), 1379–1389.
- (65) Kantorek, M.; Jesionek, K.; Polesek-Karczewska, S.; Ziolkowski, P.; Stajnke, M.; Badur, J. Thermal Utilization of Meat-and-Bone Meal Using the Rotary Kiln Pyrolyzer and the Fluidized Bed Boiler – The Performance of Pilot-Scale Installation. *Renewable Energy* **2021**, *164*, 1447–1456.
- (66) Huang, J.; Wang, Z.; Qiao, Y.; Wang, B.; Yu, Y.; Xu, M. Transformation of Nitrogen during Hydrothermal Carbonization of Sewage Sludge: Effects of Temperature and Na/Ca Acetates Addition. *Proc. Combust. Inst.* **2021**, *38*, 4335 DOI: 10.1016/j.proci.2020.06.075.
- (67) Reza, M. T.; Wirth, B.; Lüder, U.; Werner, M. Behavior of Selected Hydrolyzed and Dehydrated Products during Hydrothermal Carbonization of Biomass. *Bioresour. Technol.* **2014**, *169*, 352–361.
- (68) Wang, F.; Wang, J.; Gu, C.; Han, Y.; Zan, S.; Wu, S. Effects of Process Water Recirculation on Solid and Liquid Products from Hydrothermal Carbonization of Laminaria. *Bioresour. Technol.* **2019**, *292* (2), No. 121996.